

5-12-2014

## Defect Levels in $\text{Cu}_2\text{ZnSn}(\text{S}_x\text{Se}_{1-x})_4$ Solar Cells Probed by Current-Mode Deep Level Transient Spectroscopy

S. Das

S. K. Chaudhuri

R. N. Bhattacharya

K. C. Mandal

University of South Carolina - Columbia, mandalk@enr.sc.edu

Follow this and additional works at: [https://scholarcommons.sc.edu/elct\\_facpub](https://scholarcommons.sc.edu/elct_facpub)



Part of the [Power and Energy Commons](#)

---

### Publication Info

Published in *Applied Physics Letters*, Volume 104, Issue 19, 2014, pages 192106-1-192106-4.

© Applied Physics Letters 2014, American Institute of Physics

Das, S., Chaudhuri, S. K., Bhattacharya, R. N., & Mandal, K. C. (12 May 2014). Defect levels in  $\text{Cu}_2\text{ZnSn}(\text{S}_x\text{Se}_{1-x})_4$  solar cells probed by current-mode deep level transient spectroscopy. *Applied Physics Letters*, 104(19), #192106.

<http://dx.doi.org/10.1063/1.4876925>

<http://scitation.aip.org/content/aip/journal/apl/104/19/10.1063/1.4876925>

This Article is brought to you by the Electrical Engineering, Department of at Scholar Commons. It has been accepted for inclusion in Faculty Publications by an authorized administrator of Scholar Commons. For more information, please contact [digres@mailbox.sc.edu](mailto:digres@mailbox.sc.edu).



## Defect levels in $\text{Cu}_2\text{ZnSn}(\text{S}_x\text{Se}_{1-x})_4$ solar cells probed by current-mode deep level transient spectroscopy

Sandip Das, Sandeep K. Chaudhuri, Raghu N. Bhattacharya, and Krishna C. Mandal

Citation: [Applied Physics Letters](#) **104**, 192106 (2014); doi: 10.1063/1.4876925

View online: <http://dx.doi.org/10.1063/1.4876925>

View Table of Contents: <http://scitation.aip.org/content/aip/journal/apl/104/19?ver=pdfcov>

Published by the [AIP Publishing](#)

---

### Articles you may be interested in

[Generalized current-voltage analysis and efficiency limitations in non-ideal solar cells: Case of  \$\text{Cu}\_2\text{ZnSn}\(\text{S}\_x\text{Se}\_{1-x}\)\_4\$  and  \$\text{Cu}\_2\text{Zn}\(\text{SnyGe}\_{1-y}\)\(\text{S}\_x\text{Se}\_{1-x}\)\_4\$](#)

[J. Appl. Phys.](#) **115**, 234504 (2014); 10.1063/1.4882119

[Improving the conversion efficiency of  \$\text{Cu}\_2\text{ZnSnS}\_4\$  solar cell by low pressure sulfurization](#)

[Appl. Phys. Lett.](#) **104**, 141101 (2014); 10.1063/1.4870508

[Admittance spectroscopy of  \$\text{Cu}\_2\text{ZnSnS}\_4\$  based thin film solar cells](#)

[Appl. Phys. Lett.](#) **100**, 233504 (2012); 10.1063/1.4726042

[Structural and elemental characterization of high efficiency  \$\text{Cu}\_2\text{ZnSnS}\_4\$  solar cells](#)

[Appl. Phys. Lett.](#) **98**, 051912 (2011); 10.1063/1.3543621

[Thermally evaporated  \$\text{Cu}\_2\text{ZnSnS}\_4\$  solar cells](#)


[Appl. Phys. Lett.](#) **97**, 143508 (2010); 10.1063/1.3499284


---


A promotional banner for Applied Physics Letters featuring the journal's logo and the text 'Meet The New Deputy Editors'. Below the text are three circular headshots of the new deputy editors: Alexander A. Balandin, Qing Hu, and David L. Price.

**AIP | Applied Physics Letters**

**Meet The New Deputy Editors**

 Alexander A. Balandin

 Qing Hu

 David L. Price

## Defect levels in $\text{Cu}_2\text{ZnSn}(\text{S}_x\text{Se}_{1-x})_4$ solar cells probed by current-mode deep level transient spectroscopy

Sandip Das,<sup>1</sup> Sandeep K. Chaudhuri,<sup>1</sup> Raghu N. Bhattacharya,<sup>2</sup> and Krishna C. Mandal<sup>1,a)</sup>

<sup>1</sup>Department of Electrical Engineering, University of South Carolina, Columbia, South Carolina 29208, USA

<sup>2</sup>National Renewable Energy Laboratory, 1617 Cole Boulevard, Golden, Colorado 80401, USA

(Received 9 April 2014; accepted 3 May 2014; published online 14 May 2014)

Defect levels in kesterite  $\text{Cu}_2\text{ZnSn}(\text{S},\text{Se})_4$  (CZTSSe) solar cells have been investigated by current-mode deep level transient spectroscopy. Experiments were carried out on two CZTSSe cells with photoconversion efficiencies of 4.1% and 7.1% measured under AM 1.5 illumination. The absorber layer of the 4.1% efficiency cell was prepared by annealing evaporated ZnS/Cu/Sn stacked precursor under S/Se vapor, while the absorber of the 7.1% efficiency cell was prepared by co-evaporation of the constituent elements. The 4.1% efficiency CZTSSe cell with a S/(S + Se) ratio of 0.58 exhibited two dominant deep acceptor levels at  $E_v + 0.12$  eV, and  $E_v + 0.32$  eV identified as  $\text{Cu}_{\text{Zn}}(-/0)$  and  $\text{Cu}_{\text{Sn}}(2-/-)$  antisite defects, respectively. The 7.1% efficiency cell with purely Se composition S/(S + Se) = 0 showed only one shallow level at  $E_v + 0.03$  eV corresponding to Cu-vacancy ( $V_{\text{Cu}}$ ). Our results revealed that  $V_{\text{Cu}}$  is the primary defect center in the high-efficiency kesterite solar cell in contrast to the detrimental  $\text{Cu}_{\text{Zn}}$  and  $\text{Cu}_{\text{Sn}}$  antisites found in the low efficiency CZTSSe cells limiting the device performance. © 2014 AIP Publishing LLC. [<http://dx.doi.org/10.1063/1.4876925>]

Copper-based  $\text{I}_2\text{-II-IV-VI}_4$  quaternary kesterites— $\text{Cu}_2\text{ZnSnS}_4$  (CZTS),  $\text{Cu}_2\text{ZnSnSe}_4$  (CZTSe), and mixed chalcogen  $\text{Cu}_2\text{ZnSn}(\text{S}_x\text{Se}_{1-x})_4$  (CZTSSe) have recently emerged as the most promising absorber material system<sup>1–8</sup> alternative to  $\text{CuIn}_x\text{Ga}_{1-x}\text{Se}_2$  and CdTe absorbers in thin-film solar cells which comprise of scarce, highly expensive, and toxic elements. With a tunable direct bandgap of 1.0–1.5 eV and a large absorption coefficient ( $\alpha > 10^4 \text{ cm}^{-1}$ ),<sup>1–8</sup> the Shockley-Queisser photon balance calculations predict the theoretical efficiency limit for a single junction CZTSSe solar cell to be as high as 32.2%.<sup>9</sup> One of the major factors restricting the efficiency of polycrystalline thin-film solar cells is the presence of deep-lying electronic trap levels in the bulk of the absorber layer and interfacial states localized at the heterojunction hindering the charge transport. Kesterite solar cells are far more vulnerable to have large number of such defects in the absorber film compared to the chalcopyrites as the stability of single phase stoichiometric CZTSSe could only be found at a much narrower region in the three-dimensional ( $\mu_{\text{Cu}}-\mu_{\text{Zn}}-\mu_{\text{Sn}}$ ) chemical potential space<sup>10</sup> and the  $\text{Cu}_2\text{S}(\text{Se})-\text{ZnS}(\text{Se})-\text{SnS}(\text{Se})_2$  ternary phase diagram.<sup>11–14</sup> Theoretical studies based on density functional theory/first principle calculations have predicted various intrinsic point defects including vacancies ( $V_{\text{Cu}}$ ,  $V_{\text{Zn}}$ ,  $V_{\text{Sn}}$ , and  $V_{\text{S}}$ ), antisites ( $\text{Cu}_{\text{Zn}}$ ,  $\text{Zn}_{\text{Cu}}$ ,  $\text{Cu}_{\text{Sn}}$ ,  $\text{Sn}_{\text{Cu}}$ ,  $\text{Zn}_{\text{Sn}}$ , and  $\text{Sn}_{\text{Zn}}$ ), interstitials ( $\text{Cu}_i$ ,  $\text{Zn}_i$ , and  $\text{Sn}_i$ ), and several defect complexes (e.g.,  $[\text{Cu}_{\text{Zn}}^- + \text{Zn}_{\text{Cu}}^+]$ ,  $[\text{V}_{\text{Cu}}^- + \text{Zn}_{\text{Cu}}^+]$ , etc.) that may exist in CZTSSe depending on its composition.<sup>15–20</sup> However, there exists meagre information on the experimental identification of such electrically active defects in CZTSSe solar cells. In this Letter, we report on the investigation of the deep levels in CZTSSe

solar cells probed by current-mode deep level transient spectroscopy (I-DLTS) to quantify the trap activation energies ( $E_T$ ), trap concentrations ( $N_T$ ), and capture cross-sections of the traps ( $\sigma_T$ ).

The conventional capacitive DLTS (C-DLTS) technique is a very sensitive tool to identify electrically active defects in semiconductors in terms of activation energy, defect type, and trap concentration<sup>21</sup> and have been widely used for deep and shallow level defect characterization of chalcopyrites and chalcogenides.<sup>22,23</sup> The CZTSSe cells under investigation exhibited large depletion capacitance ( $C_d$ ) beyond the detection limit of our DLTS system and therefore we have used I-DLTS technique which uses current transient measurements to identify the defect levels. Although, unlike C-DLTS, I-DLTS cannot distinguish between a majority and minority carrier trap, but it provides valuable information relating to the defect activation energies, defect concentration, and the capture cross-sections of the defect centers.

We have performed I-DLTS measurements on two different  $\text{Cu}_2\text{ZnSn}(\text{S}_x\text{Se}_{1-x})_4$  cells in this study, namely, Cell 1 and Cell 2, with Cell 1 having a S/Se ratio of 1.4 ( $x = \text{S}/(\text{S} + \text{Se}) = 0.58$ ), and Cell 2 containing purely Se ( $x = 0$ ). The absorber layer of Cell 1 was prepared by a two-step process: deposition of ZnS/Cu/Sn precursor stacked layer on Mo-coated soda lime glass (SLG) substrates by sequential thermal evaporation followed by annealing under S + Se vapor in a tube furnace. The pure CZTSe absorber of Cell 2 was prepared by co-evaporation of the constituent elements.<sup>3</sup> The finished CZTSSe solar cells had a SLG/Mo/p-CZTSSe/n-CdS/i-ZnO/Al:ZnO/Al device structure. The J-V characteristics of the two cells under dark and under simulated AM 1.5 illumination are shown in Fig. 1. Cell 1 showed a higher open-circuit voltage ( $V_{\text{OC}}$ ) of 506 mV compared to Cell 2, which exhibited a maximum  $V_{\text{OC}} = 350$  mV at 297 K. Both cells were

<sup>a)</sup>Author to whom correspondence should be addressed. Electronic mail: mandalk@cec.sc.edu

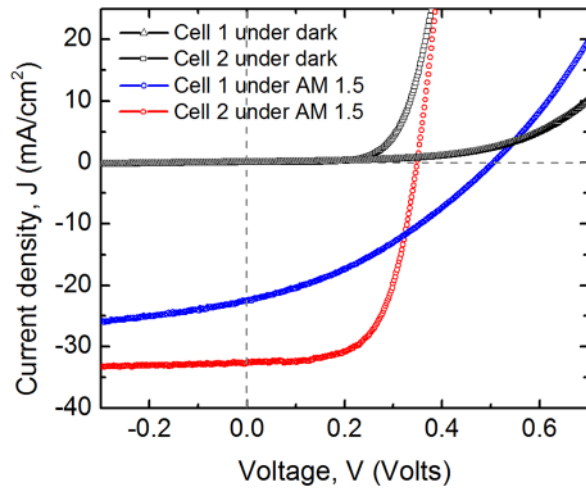


FIG. 1. J-V characteristics of the cells under dark and under AM 1.5 simulated illumination.

Cu-poor in composition and had a slightly Zn-rich stoichiometry. The compositional details, thickness and bandgaps of the absorber layers for the two cells are listed in Table I. The photovoltaic and electrical parameters of the two cells under investigation are summarized in Table II.

A SULA DDS-12 DLTS system was operated in current transient spectroscopy (CTS) mode to obtain the I-DLTS spectra. Schematic of the experimental set-up is represented in Fig. 2. The samples were mounted on a JANIS VPF800 cryostat stage controlled by a Lakeshore 335 temperature controller. The cells were reverse biased at  $V_R = -0.4$  V and a trap filling forward pulse of amplitude  $V_a = +0.3$  V with 10 ms pulse width was applied following which the current transients were recorded. The transient signals were successively processed by the CTS unit and the I-DLTS spectra were generated by choosing a suitable rate window using the correlator units to calculate the emission rates at different temperatures following the standard double boxcar method. The correlator unit in DDS-12 is capable of assigning multiple rate windows in a single thermal scan. From Eq. (1) given below,<sup>24</sup> it can be seen that the expression of the current transient in I-DLTS also contains the steady-state diode leakage current

$$i(t) = \frac{qWA}{2\tau_{e,h}} N_T(t) + I_L, \quad (1)$$

where  $q$  is the electronic charge,  $W$  is the width of the measurement volume,  $A$  is the diode area,  $\tau_{e,h}$  is the decay constant for the current transients corresponding to electron or hole emissions, and  $N_T$  is the concentration of trapped charge carriers. If the diode leakage current exceeds a certain limit it can obscure the current transients. The correlator unit also removes the background leakage current prior to the measurements to avoid any such issues. The current transient

TABLE I. Summary of the absorber layer composition and bandgaps for the two cells under investigation.

Cell ID	Type of conductivity	$\frac{Cu}{(Zn+Sn)}$	$\frac{Zn}{Sn}$	$\frac{S}{(S+Se)}$	Absorber thickness ( $\mu\text{m}$ )	$E_g$ (eV)
Cell 1	p-type	0.77	1.13	0.58	1.3	1.3
Cell 2	p-type	0.84	1.15	0.0	1.5	1.0

captures were time delayed after the end of each filling pulse by an amount called the *initial delay*. The rate windows  $\tau$  for the transient capture are dependent on the *initial delays* in the following way

$$\tau = \frac{1}{(1.94 \times \text{initial delay (ms)})}. \quad (2)$$

The capture cross-sections and the trap concentration were calculated from the I-DLTS plots. The activation energies ( $E_T$ ) of the deep centers were extracted from the Arrhenius plots obtained from the emission rates calculated from the current transients.

The I-DLTS scans of Cell 1 and Cell 2 in the temperature range of 85–325 K are shown in Figs. 3(a) and 3(b), respectively. It can be readily observed that the defect characteristics in these two cells are quite different. For Cell 1, two broad peaks were noticed, one close to 190 K (peak 1) and the other one close to 285 K (peak 2) for the lowest *initial delay* of 0.1 ms. Such broad peaks signify a slow emission rate of the defect centers. Interestingly, none of these two peaks were observed in Cell 2, rather a new peak (peak 3) appeared close to 100 K (for an *initial delay* of 0.02 ms) which is much narrower signifying a faster emission of trapped carriers from the associated defect center.

The Arrhenius plots corresponding to the observed peaks in the I-DLTS scan are shown in Fig. 4. Activation energies of  $E_{T1} = 0.12$  eV and  $E_{T2} = 0.32$  eV were extracted corresponding to peaks 1 and 2, respectively. Due to the broad distribution of the emission rates, the uncertainties in the activation energies in Cell 1 were estimated to be  $\pm 0.04$  for  $E_{T1}$  and  $\pm 0.06$  eV for  $E_{T2}$ . An activation energy of  $E_{T3} = 0.03 \pm 0.01$  eV was calculated corresponding to the peak 3 in Cell 2.

Recent theoretical analysis of defect models in kesterite CZTS and CZTSe materials<sup>10,15–20</sup> have been considered to assign the experimentally observed defect levels in this study. Nagoya *et al.*,<sup>15</sup> Maeda *et al.*,<sup>16,17</sup> and Chen and co-workers<sup>10,18–20</sup> have carried out systematic theoretical studies on the intrinsic point defects in CZTS/CZTSe and calculated the formation energies and corresponding transition (activation) energies for various point defects. It is predicted that the acceptor defects ( $\text{Cu}_{Zn}$ ,  $\text{V}_{Cu}$ ,  $\text{Zn}_{Sn}$ ,  $\text{V}_{Zn}$ ,  $\text{Cu}_{Sn}$ , etc.) have much lower energy of formation compared to the donor

TABLE II. Electrical and photovoltaic performance parameters of Cell 1 and Cell 2.

Cell ID	Area ( $\text{cm}^2$ )	$V_{OC}$ (mV)	$J_{SC}$ ( $\text{mA}/\text{cm}^2$ )	FF (%)	Efficiency, $\eta$ (%)	Ideality factor, n	Series resistance ( $\Omega$ )	Shunt resistance ( $\Omega$ )
Cell 1	0.42	506	22.5	35	4.1	4.5	31.2	125
Cell 2	0.43	350	32.7	62	7.1	1.4	5.06	357

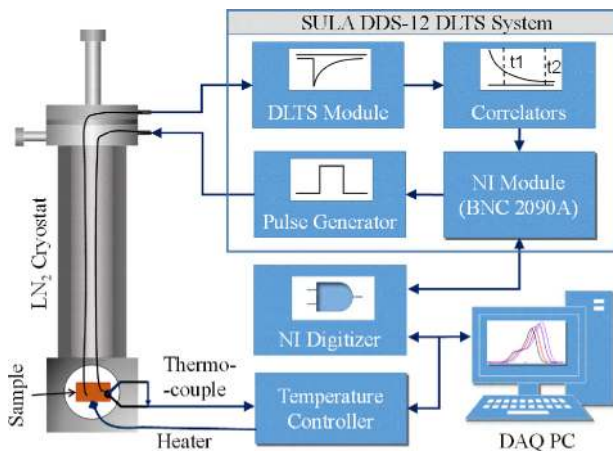


FIG. 2. Schematic of the I-DLTS experimental setup.

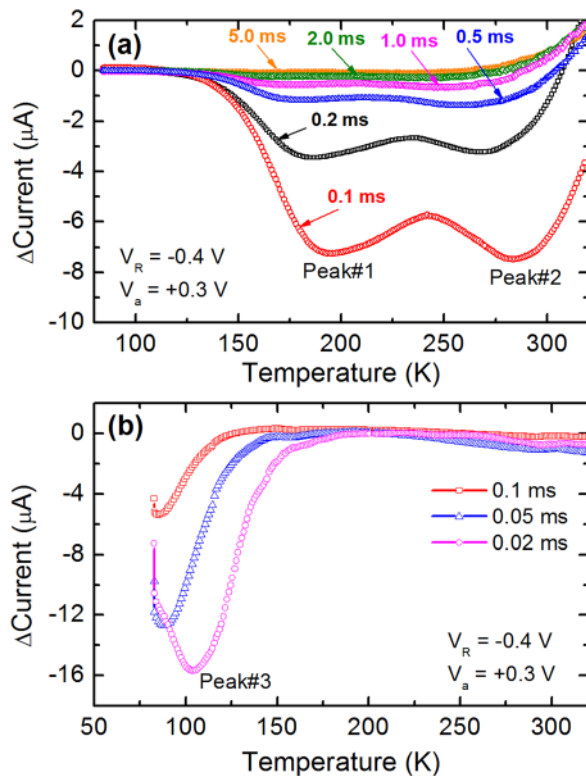


FIG. 3. I-DLTS signal of (a) Cell 1 and (b) Cell 2.

defects in these material systems for Cu-poor composition. The  $\text{Cu}_{\text{Zn}}$  antisite defect has the lowest formation energy which acts as an acceptor level located about 0.10–0.15 eV above the valence band maxima (VBM)<sup>18–20</sup> and is considered to be responsible for the intrinsic p-type conductivity of these materials. The copper vacancy ( $\text{V}_{\text{Cu}}$ ) has comparatively higher energy of formation than  $\text{Cu}_{\text{Zn}}$  antisite and

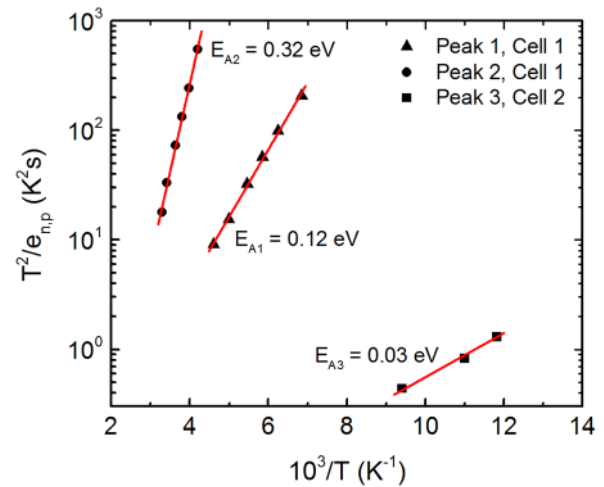


FIG. 4. Arrhenius plots corresponding to the peaks obtained from I-DLTS spectra shown in Fig. 3. The solid straight lines show the linear fit to the experimental data points.

contributes to a much shallower acceptor level at  $\sim 0.02$  eV above the VBM.<sup>18</sup> It is suggested that  $\text{V}_{\text{Cu}}$  is much preferable than the  $\text{Cu}_{\text{Zn}}$  antisite for high performance solar cells, since  $\text{Cu}_{\text{Zn}}$  produces deeper acceptor level than  $\text{V}_{\text{Cu}}$  and is thus detrimental to the cell performance. Existence of  $\text{Cu}_{\text{Zn}}$  deep level at  $E_{\text{v}} + 0.12$  eV has also been experimentally identified by admittance spectroscopy.<sup>25</sup>

The theoretical studies strongly suggest that the observed trap level  $E_{\text{T}1}$  in Cell 1 with an activation energy of 0.12 eV can be assigned to the  $\text{Cu}_{\text{Zn}}(-/0)$  antisite defect. The second dominant defect level identified in Cell 1 ( $E_{\text{T}2}$ ) corresponds to a much deeper level with an activation energy of 0.32 eV which matches closely to the transition energy theoretically calculated for  $\text{Cu}_{\text{Sn}}(2-/)$  defect.<sup>19,20</sup> The larger capture cross-section of  $E_{\text{T}2}$  compared to that of  $E_{\text{T}1}$  also suggests that  $E_{\text{T}2}$  has a more negatively charged state. Therefore, we attribute the deep level at  $E_{\text{v}} + 0.32$  eV to the  $\text{Cu}_{\text{Sn}}(2-/)$  antisite defect.

In Cell 2, the activation energy of trap level  $E_{\text{T}3} = 0.03$  eV can be assigned to the copper vacancy ( $\text{V}_{\text{Cu}}$ ), as no other shallow level in this range exists in these materials. The experimentally identified value of  $E_{\text{v}} + 0.03$  eV is in good agreement with the theoretical predicted value of 0.02 eV. All the experimentally identified defect parameters including the defect activation energy ( $E_{\text{T}}$ ), capture cross-section ( $\sigma_{\text{T}}$ ), trap concentration ( $N_{\text{T}}$ ), and the associated point defects are summarized in Table III.

We would like to emphasize that a device having shallow defect levels is expected to exhibit superior performance than a device with deeper defect levels. Our results follow this trend with Cell 2 showing much better photovoltaic

TABLE III. Summary of the observed defect levels in the CZTSSe solar cells by I-DLTS.

Cell ID	Peak ID	Approx. peak temperature (K)	Activation energy, $E_{\text{T}}$ (eV)	Capture cross section, $\sigma_{\text{T}}$ ( $\text{cm}^2$ )	Trap conc. $N_{\text{T}}$ ( $\text{cm}^{-3}$ )	Possible defect level
Cell 1	Peak 1	190	$0.12 \pm 0.04$	$1.31 \times 10^{-20}$	$6.17 \times 10^{14}$	$\text{Cu}_{\text{Zn}}$
	Peak 2	285	$0.32 \pm 0.06$	$2.04 \times 10^{-18}$	$6.73 \times 10^{14}$	$\text{Cu}_{\text{Sn}}$
Cell 2	Peak 3	100	$0.03 \pm 0.01$	$2.52 \times 10^{-20}$	$6.46 \times 10^{15}$	$\text{V}_{\text{Cu}}$

performance compared to Cell 1. However, the most interesting observation in this study is the presence of shallow  $V_{Cu}$  level in purely Se containing CZTSe sample (Cell 2) which suggests that although  $Cu_{Zn}$  has a lower formation energy, it is possible to have  $V_{Cu}$  as the predominant lattice defect in kesterites. Our results also indicate that the intrinsic p-type conductivity of high-efficiency CZTSSe absorbers could be due to the formation of copper vacancies ( $V_{Cu}$ ) similar to chalcopyrites and the formation of detrimental  $Cu_{Zn}$  antisites can be avoided.

In conclusion, we have performed current DLTS measurements on two Cu-poor and Zn-rich CZTSSe solar cells with different chalcogen ratios to probe electrically active intrinsic point defects. The lower efficiency CZTSSe cell ( $S/Se = 1.4$ ) showed two dominant deep acceptor levels at  $E_v + 0.12$  eV and  $E_v + 0.32$  eV corresponding to  $Cu_{Zn}$  and  $Cu_{Sn}$  antisites, whereas the pure CZTSe ( $S/Se = 0$ ) higher efficiency cell showed only a shallow  $V_{Cu}$  level at  $E_v + 0.03$  eV. Our investigation suggests that  $V_{Cu}$  could be the predominant lattice defect in high efficiency kesterite cells instead of the detrimental  $Cu_{Zn}$  antisites.

We would like to thank Ingrid Repins (NREL) for providing us with physical vapor deposited CZTSe sample. One of the authors (R. N. Bhattacharya, NREL) would like to acknowledge partial financial support from “Alliance for Sustainable Energy, LLC,” under Contract No. DE-AC36-08GO28308 with the U.S. Department of Energy (LDRD program).

<sup>1</sup>T. K. Todorov, J. Tang, S. Bag, O. Gunawan, T. Gokmen, Y. Zhu, and D. B. Mitzi, *Adv. Energy Mater.* **3**, 34 (2013).

<sup>2</sup>S. Bag, O. Gunawan, T. Gokmen, Y. Zhu, T. K. Todorov, and D. B. Mitzi, *Energy Environ. Sci.* **5**, 7060 (2012).

- <sup>3</sup>I. Repins, C. Beall, N. Vora, C. DeHart, D. Kuciauskas, P. Dippo, B. To, J. Mann, W.-C. Hsu, A. Goodrich, and R. Noufi, *Sol. Energy Mater. Sol. Cells* **101**, 154 (2012).
- <sup>4</sup>K. Wang, O. Gunawan, T. Todorov, B. Shin, S. J. Chey, N. A. Bojarczuk, D. Mitzi, and S. Guha, *Appl. Phys. Lett.* **97**, 143508 (2010).
- <sup>5</sup>Q. Guo, G. M. Ford, W.-C. Yang, B. C. Walker, E. A. Stach, H. W. Hillhouse, and R. Agrawal, *J. Am. Chem. Soc.* **132**, 17384 (2010).
- <sup>6</sup>H. Katagiri, N. Sasaguchi, S. Hando, S. Hoshino, J. Ohashi, and T. Yokota, *Sol. Energy Mater. Sol. Cells* **49**, 407 (1997).
- <sup>7</sup>S. Das and K. C. Mandal, in *Proceedings of 38th IEEE Photovoltaic Specialists Conference (PVSC)* (Austin, Texas, 2012), p. 002668.
- <sup>8</sup>R. N. Bhattacharya, *Open Surf. Sci. J.* **5**, 21 (2013).
- <sup>9</sup>W. Shockley and H. J. Queisser, *J. Appl. Phys.* **32**, 510 (1961).
- <sup>10</sup>S. Chen, X. G. Gong, A. Walsh, and S.-H. Wei, *Appl. Phys. Lett.* **96**, 021902 (2010).
- <sup>11</sup>I. D. Oleksyuk, I. V. Dudchar, and L. V. Piskach, *J. Alloys Compd.* **368**, 135 (2004).
- <sup>12</sup>I. V. Dudchak and L. V. Piskach, “Phase equilibria in the  $Cu_2SnSe_3$ - $SnSe_2$ - $ZnSe$  system,” *J. Alloys Compd.* **351**, 145 (2003).
- <sup>13</sup>S. Das, R. M. Krishna, S. Ma, and K. C. Mandal, *J. Cryst. Growth* **381**, 148 (2013).
- <sup>14</sup>S. Das and K. C. Mandal, *Jpn. J. Appl. Phys.* **52**, 125502 (2013).
- <sup>15</sup>A. Nagoya, R. Asahi, R. Wahl, and G. Kresse, *Phys. Rev. B* **81**, 113202 (2010).
- <sup>16</sup>T. Maeda, S. Nakamura, and T. Wada, *Thin Solid Films* **519**, 7513 (2011).
- <sup>17</sup>T. Maeda, S. Nakamura, and T. Wada, *Jpn. J. Appl. Phys.* **50**, 04DP07 (2011).
- <sup>18</sup>S. Chen, J.-H. Yang, X. G. Gong, A. Walsh, and S.-H. Wei, *Phys. Rev. B* **81**, 245204 (2010).
- <sup>19</sup>S. Chen, A. Walsh, X.-G. Gong, and S.-H. Wei, *Adv. Mater.* **25**, 1522 (2013).
- <sup>20</sup>A. Walsh, S. Chen, S. Wei, and X. Gong, *Adv. Energy Mater.* **2**, 400 (2012).
- <sup>21</sup>D. V. Lang, *J. Appl. Phys.* **45**, 3023 (1974).
- <sup>22</sup>L. L. Kerr, S. S. Li, S. W. Johnston, T. J. Anderson, O. D. Crisalle, W. K. Kim, J. Abushama, and R. N. Noufi, *Solid-State Electron.* **48**, 1579 (2004).
- <sup>23</sup>M. A. Lourenço, Y. K. Yew, K. P. Homewood, K. Durose, H. Richter, and D. Bonnet, *J. Appl. Phys.* **82**, 1423 (1997).
- <sup>24</sup>J. A. Borsuk and R. M. Swanson, *IEEE Trans. Electron Devices* **27**, 2217 (1980).
- <sup>25</sup>E. Kask, T. Raadik, M. Grossberg, R. Josepson, and J. Krustok, *Energy Procedia* **10**, 261 (2011).